Prediction of the functional properties of ceramic materials from composition using artificial neural networks

D. J. Scott [a], P. V. Coveney [a,*], J. A. Kilner [b], J. C. H. Rossiny [b], N. Mc N. Alford [c]

[a] *Centre for Computational Science, Department of Chemistry, University College London, Christopher Ingold Laboratories, 20 Gordon Street, London, WC1H 0AJ*

[b] *Department of Materials, Imperial College London, Exhibition Road, London, SW7 2AZ*

[c] *Centre for Physical Electronics and Materials, Faculty of Engineering, Science and the Built Environment, London South Bank University, 103 Borough Road, London, SE1 0AA*

Abstract

We describe the development of artificial neural networks (ANN) for the prediction of the properties of ceramic materials. The ceramics studied here include polycrystalline, inorganic, non-metallic materials and are investigated on the basis of their dielectric and ionic properties. Dielectric materials are of interest in telecommunication applications where they are used in tuning and filtering equipment. Ionic and mixed conductors are the subjects of a concerted effort in the search for new materials that can be incorporated into efficient, clean electrochemical devices of interest in energy production and greenhouse gas reduction applications. Multi-layer perceptron ANNs are trained using the back-propagation algorithm and utilise (利用) data obtained from the literature to learn composition-property relationships between the inputs and outputs of the system. The trained networks use compositional information to predict the relative permittivity (介电常数) and oxygen diffusion properties of ceramic (陶瓷) materials. The results show that ANNs are able to produce accurate predictions of the properties of these ceramic materials which can be used to develop materials suitable for use in telecommunication and energy production applications.

Key words: C. Dielectric properties, C. ionic conductivity, D. perovskites, E. functional applications, neural networks

1 Introduction

Accurate determination of the properties of a ceramic [1] material allows it to be matched to appropriate applications and therefore, fast and reliable methods for predicting material properties would be extremely useful. Various modelling techniques can be used to predict material properties from compositional and processing information and can provide fast and accurate results. In the conventional "Popperian" scientific method [2], a theory is proposed and tested by experiment. Whilst such experiments increase our confidence in the model, one experiment can falsify the theory which can never have more than a provisional status. Inductive "Baconian" methods [3], in contrast to the Popperian technique, begin with experiment and use statistical inference to develop a model. In principle, such techniques make no prior assumptions about an underlying theoretical model and utilise statistical methods to induce data relationships.

Popperian modelling of the properties of ceramic materials has yielded important results. Models of the diffusion of oxygen through mixed ionic conductors [4] have provided accurate predictions of the diffusion coefficient; likewise, successful modelling of the structure-performance relationship of solid oxide fuel cell (SOFC) electrodes has been performed [5]. Prediction of the grain boundary properties of dielectric ceramic materials has also been performed [6]. In this paper, by contrast, we attempt to produce a Baconian model capable of predicting properties of a wide range of ceramic materials. It would be extremely difficult to develop such a model using conventional (Popperian) techniques [7] and therefore, we use the inductive approach known as an artificial neural network (ANN).

ANNs are one of several "biologically inspired" computational methods which can be used to capture complex, non-linear relationships between data [8]. These techniques have been used in many areas of chemistry [7] and have provided accurate predictions in the performance of oil-field cements [9] and materials with highly complex behaviour [10]. It is generally accepted that ANNs provide more accurate predictive capabilities than methods based on traditional linear or non-linear statistical regression [11] and the superiority of ANNs over regression techniques increases as the dimensionality and/or non-linearity of the problem increases [12]. ANNs have been found to outperform regression techniques in the prediction of ceramic material properties [13,14,15,16]. Additionally, the prediction of dielectric properties of organic materials has been attempted [17] and, again, ANNs have been found to be superior.

* Corresponding author

In previously published work, compositional information has formed the core of the ANN input data although other descriptors can be added to the model to help improve performance [18,19]. Whilst accurate prediction of ceramic material properties has been performed previously, this is often based on one material, to which dopants are applied. Here we have attempted property prediction of a much wider range of materials than completed previously. Materials in our datasets range from single compounds, through to complex binary, ternary and quaternary systems. The large range of materials studied requires statistical techniques capable of handling high-dimensional problems; ANNs are ideally suited for this purpose. With an automated combinatorial robotic instrument such as the London University Search Instrument (LUSI) [20] we can use ANNs to rapidly scan compositional parameter space, searching for desirable materials.

2 Electroceramic materials

The study of ceramic materials is a wide ranging and complex subject due to both the large range of materials available and the varied properties exhibited [21]. In our own work, we are interested in dielectric ceramics for use in communications equipment and oxygen diffusion properties of ceramics for fuel cells components. The continuing growth of mobile telecommunications has sustained the interest in novel ceramics for use as dielectric resonators (DRs) at microwave frequencies (1-20 GHz). New materials are constantly required for use in resonators and filters. Additionally, ion-diffusing ceramics are employed in a wide range of applications. In particular, electrochemical devices such as oxygen separation membranes, solid oxide fuel cell (SOFC) cathodes, and syngas reactors make use of the ion-diffusion properties of ceramic materials.

One of the most promising classes of materials suitable for use in such applications are the perovskite oxides with the general formula ABO_3. A and B are rare earth/alkaline earth ions and transition metal cations, respectively. By doping both the A- and B-sites with similar metallic elements, the composition of these materials can be broadened to encompass a very large number of possible combinations. Dopant species and compositions can have a major effect on the properties of the material.

Due to the difficult and time consuming process of conventional compound synthesis, scientists are increasingly turning to high-throughput combinatorial techniques to develop suitable materials [22,23]. Combinatorial projects can generate vast quantities of data which require informatics and database systems [20] for data entry, organisation and data mining. Our Functional Oxide Discovery (FOXD) project, which is based around LUSI,

aims to utilise artificial neural network data analysis techniques to complete the "materials discovery cycle", allowing the predictions made to direct the search for new materials into as yet unexplored territory [20,24].

2.1 Microwave dielectric materials for communications equipment

The ideal properties of a dielectric resonator (DR) are a sufficiently high relative permittivity to allow miniaturisation of the component ($\epsilon_r > 10$) and high 'Q' factor at microwave frequencies to improve selectivity (Q > 5000). The quality factor, Q is given by the inverse of the dissipation factor $Q = 1/\tan\delta$ where δ is the *loss angle*, the phase shift between the voltage and current when an AC field is applied to a dielectric material. [25].

Many useful dielectric resonator materials are perovskites (e.g. (Ba,Sr)TiO_3, (Ba,Mg)TaO_3, 0.7$CaTiO_3$-0.3$NdAlO_3$ and Ba(Zn,Nb)O_3). Whilst the barium strontium titanate system ($Ba_{1-x}Sr_xTiO_3$) has been examined in detail experimentally [26,27,28,29], it has not been manufactured and tested over the complete range from pure $BaTiO_3$ to pure $SrTiO_3$. The present paper describes the development of an ANN capable of predicting the relative permittivity of barium strontium titanate along with many other perovskite materials.

Guo *et al*. have previously investigated the use of ANNs for the prediction of the properties of dielectric ceramics such as $BaTiO_3$ [13] etc. Their work concentrated on the effect of the addition of other compounds (lanthanum oxide, niobium oxide, samarium oxide, cobalt oxide and lithium carbonate) to pure barium titanate. Other work by Schweitzer *et al*. [19] attempted prediction of dielectric data listed in the *CRC Handbook* and the *Handbook of Organic Chemistry*. This work used molecular information such as topological (bond type, number of occurrences of a structural fragment or functional group) and geometric (moment of inertia, molecular volume, surface area) descriptors in addition to the compositional information as the input variables. Additionally, there has been considerable work aimed at predicting the electrical properties of lead zirconium titanate (PZT) using ANN techniques [16,30,31]. PZT is a piezoelectric ceramic material which finds increasing application in actuators and transducers.

2.2 Ion-diffusion materials for fuel cells

As noted above, ion-conducting ceramics are used in electrochemical devices such as oxygen separation membranes, solid oxide fuel cell (SOFC) cathodes and syngas reactors. Solid oxide fuel cells are of great interest as

economical, clean and efficient power generation devices [32]. Fuel cells have several advantages over conventional power generation techniques including their high-energy conversion efficiency and high power density while engendering extremely low pollution, in addition to the flexibility they confer in the use of hydrocarbon fuel [33]. Traditionally, large scale SOFCs have been based on yttria stabilised zirconia (YSZ) electrolytes and operate at high temperature (1000°), placing considerable restrictions on the materials that can be used. Reduction of the operating temperature is essential for the future successful development of SOFCs, allowing increased reliability and the use of a wider range of materials.

SOFC cathodes have stringent requirements. Ideally, the cathode material should be stable in an oxidising environment, have a high electrical conductivity, be thermally and chemically compatible with the other components of the cell and have sufficient porosity to allow gas transport to the oxidation site. Critically, the cathode material must allow diffusion of oxygen ions through the crystal lattice. The flexible perovskite structure of these materials allows doping, introducing defects into the lattice and facilitating the diffusion of ion species through the material. Materials currently under investigation include $La_{1-x}Sr_xMn_yCo_{1-y}O_3$ (LSMC) [34], $La_{1-x}Ca_xFeO_{3-\delta}$ (LCF) [35], $La_{2-x}Sr_xNiO_{4+\delta}$ (LSN) [36] and $Ba_xSr_{1-x}Co_{1-y}Fe_yO_{3-\delta}$ (BSCF) [37]. Much of the interest in these materials has stemmed from the fact that they form with oxygen deficiencies which provide a mechanism for fast oxygen ion transport through the defects in the crystal structure. Despite their ion transport properties, many possible SOFC cathode materials suffer from thermomechanical deficiencies such as cracking. Doping of Sr with other alkaline earth metals and replacing Mn, Co and Fe with other transition metals permits a wide range of possible materials allowing development of a material with optimal ion transport and thermomechanical properties [36].

There has been considerable investigation into the prediction of overall fuel cell performance using ANN techniques [38,39,40,41], and some work on the modelling of diffusion properties has also been carried out [4]. However, there has been little work on the ANN prediction of oxygen diffusion properties of the ceramic materials used as individual components of fuel cells although Ali *et al* [5] have recently investigated the structure-performance relationship of SOFC electrodes. Here, we present the results of our work on the development of ANNs for the prediction of the oxygen diffusion properties of ceramic materials. These networks may be subsequently included in the larger FOXD project [24], allowing development of optimal SOFC cathode materials.

3 Artificial neural networks

Artificial neural networks can be used to develop functional approximations to data with almost limitless application [12,42]. ANNs use existing data to learn the functional relationships between inputs and outputs. Unlike standard statistical regression techniques, ANNs make no prior assumption of the input-output relationship, a powerful advantage in their application to complex systems.

ANNs are formed from individual processing units, or *neurons*, connected together in a network. The individual units are arranged into layers and the power of the neural computation comes from the interconnection between the layers of processing units. An individual unit consists of weighted inputs, a *combination* function, an *activation* function and one output. The outputs of one layer are connected to the inputs of the next layer to form the network topology. The performance of the network is determined by the form of the activation function, the training algorithm and by the network architecture. The selection of input data and architecture is a non-trivial process [43,44] and can have a large effect on the ultimate predictive abilities of the network. The individual units operate by evaluating the combination function which transforms the input and weight vectors into a scalar value. The output of the combination function is transformed through the activation function to give the neuron's "state of activation". The use of a non-linear activation function is responsible for the ability of the network to learn non-linear functions as a whole.

For an ANN to be able to make predictions, it must be trained. The training process involves the application of a *training dataset* to the network. The training algorithm is used to iteratively adjust the network's interconnection weights so that the error in prediction of the training dataset records is minimised and the network reaches a specified level of accuracy. The network can then be used to predict output values for new input data and is said to generalise well if such predictions are found to be accurate.

3.1 Multi-layer perceptron networks

In a multi-layer perceptron (MLP) network, the individual processing units are known as *perceptrons* and they are usually arranged into three layers: input, hidden and output. Hecht-Nielsen proved that any continuous function can be approximated over a range of inputs by using a three layer feed forward neural network with back-propagation of errors [45].

The number of neurons in the input and output layers is determined by the

number of independent and dependent variables respectively. The number of hidden neurons is determined by the complexity of the problem and is often obtained by trial and error although evolutionary computing techniques such as genetic algorithms [46] have been used to determine optimal network architecture.

We now describe a feed-forward neural network with back-propagation of errors. The operation of the network is as follows:

(1) Input some data x_i to the input layer.
(2) Evaluate the combination function:

$$c_j = \sum_{i}^{N} w_{ij} x_i + \theta$$

which in this case is the *dot product* of the input vector x_i and the weights w_{ij} where j is the number of the hidden node being calculated, θ is the bias and N is the length of the input vector.
(3) Calculate the value of the hidden node by applying a tanh-sigmoid activation function

$$H_j = \frac{2}{(1 + exp(-2c_j))} - 1,$$

where j is the number of the hidden node and y is the output of the combination function defined earlier.
(4) Calculate the network's output values O_k at neuron k:

$$O_k = g' \left(\sum_{l}^{P} w'_{lk} H_l + \theta' \right),$$

where k is the number of the output node being calculated, θ' is the bias, w'_{lk} is the connection weight and P is the length of the hidden node vector (the number of hidden nodes); g' is a linear activation function.
(5) Use the difference between O_k and the data contained in the training set along with the derivative of the activation function to calculate the correction factor (δ_k) to the weights connecting the hidden and output layer neurons:
(6) Use the correction factor to calculate the actual corrections to the weights connecting the hidden and output layer neurons

$$w_{jk}^{new} = w_{jk}^{old} + \eta \delta_k H_j$$

where η is the *learning rate* and controls the adjustments to the weights/biases.

(7) Calculate the correction factors for the weights connecting the input and hidden neurons, and insert these corrections
(8) Return to the first step and repeat the algorithm with the next entry in the training dataset.

The application of this algorithm to the complete training dataset is known as an *epoch*. The network's performance is measured after each epoch has been completed and is determined by an error function. Two common error functions have been used, both based on the difference between the network's prediction and the expected values for the entire dataset. The first error function is the root mean square (RMS) of the prediction error:

$$\epsilon_{RMS} = \sqrt{\frac{\sum_{i=1}^{N}(y_i - t_i)^2}{N}}, \tag{1}$$

where y is the output predicted by the network, t is the experimentally measured output and N is the number of records in the dataset. The second error function is known as the root relative squared (RRS) error and is given by:

$$\epsilon_{RRS} = \sqrt{\frac{\sum_{i=1}^{N}(y_i - t_i)^2}{\sum_{i=1}^{N}(t_i - \overline{t})}}, \tag{2}$$

where $\overline{t}$ is the mean of the experimentally measured outputs and the other symbols have been defined previously.

The training process corresponds to an iterative decrease in the error function and continues until a predetermined value is reached, when training is halted. The trained network is tested through the application of previously unseen data to determine the performance. A network which performs well when working on new data is said to have good generalisation properties. As with statistical regression models, ANNs tend to perform much better when interpolating than extrapolating predictions. That is, whilst predictions are possible for any values of the input space, the most accurate and reliable results will be found when attempting predictions of materials which are similar to materials found in the training dataset.

The selection of the error function value at which the training process is halted is not as simple as might first appear. The obvious choice is to select a low value, to obtain as high accuracy as possible. Unfortunately, this is found to lead to *over-training*: the training dataset is "memorised" by the network and the generalisation to new data is poor. The effects of over-training occurring can be reduced by the use of another dataset, known as a *validation dataset* which is used to monitor the training process. After each

epoch of training, the network is used to predict the output values of the validation dataset and the error function (1 or 2) of the validation dataset is calculated. When training starts, the error function of the validation dataset decreases in line with the error function of the training dataset. However, as the network begins to become over-trained, the error function of the validation dataset increases, and training is halted. It is the point where the error function of the validation dataset reaches a minimum that the network is expected to have the best generalisation performance. The use of the validation dataset to help prevent over-training is known as *early stopping* [8] of the training process.

3.2 Radial basis function networks

Radial basis function (RBF) neural networks [47] operate in a similar fashion to MLP networks. The key difference is that the combination function is the *euclidean distance* between the input vector and the weight vector instead of the dot-product used in MLP networks. The most common form of basis function used is the Gaussian:

$$H_j = \exp\left(-\frac{x^2}{2\sigma^2}\right), \tag{3}$$

where x is the euclidean distance between the input vector and the centre of the Gaussian basis function and σ is a parameter which determines the "width" of the function.

RBF training algorithms operate in two stages. The first is unsupervised and uses only the input data of the training set. This stage involves the use of clustering algorithms such as K-means clustering [48] to determine suitable locations and width parameters for the basis functions. The second stage is identical to that used in MLP networks. Once the training algorithm has been used to locate the basis functions throughout parameter space and to calculate the second layer weights, the RBF network can be used to give predictions on new data. An important theoretical advantage of RBF over MLP networks is that the RBF training algorithm is the solution of a linear problem and can often be performed much faster than the complete non-linear optimisation required in the training of an MLP network.

3.3 Generalisation in artificial neural networks

The goal of ANN methods is to develop a network which is capable of accurately predicting output data values for records which are previously

unseen by the network. An estimate of the generalisation performance of a network can be obtained by calculating the error function, eqn. (1) or (2), of a dataset which is independent of that used for training. Such a dataset is known as the *test dataset*. In order to utilise all of the data available, and to ensure that network performance is not simply due to coincidental dataset selection, cross-validation analysis is performed [49]. In cross-validation, the data is divided into a number of subsets. All bar one of the datasets are employed for training/validation and the dataset withheld is used for testing. This process is repeated, each time withholding a different dataset and using the remainder for training/validation. In this way, all of the data is used for testing and the likelihood that the network performance is due to chance dataset selection is significantly reduced. Once complete, the mean of the error function from each repetition is calculated. This value is known as the *generalisation error* and provides a measure of the overall performance of the network. To further increase confidence in the generalisation error, repeated cross-validation can be performed. In repeated cross-validation, cross-validation is performed several times, randomising the data in between each cross-validation. In this way, n times m-fold cross-validation is performed, the network is trained n x m times and we can be even more confident that the quoted generalisation error is accurate.

4 Ceramic materials datasets

Our dielectric dataset contains 700 records on the composition of dielectric resonator materials and their properties [50]. Many ceramic properties such as porosity, grain size, raw materials, processing parameters, measurement techniques and even the equipment used to manufacture them can all affect the dielectric properties. Since all material properties can be affected by such parameters the inclusion of such information may increase our ability to predict ceramic material properties.

The majority of materials found in the dataset are Group II titanates, and Group II and transition metal oxides. Also included are some oxides of the lanthanides and actinides. The dataset contains relative permittivity values and Q-factors for 99% of the records. Resonant frequency and temperature coefficient of resonant frequency data are also listed, but are only available for 58% and 83% of the records respectively. The 700 records in the training dataset contain 53 different elements of which these materials may be comprised (Ag, Al, B, Ba, Bi, Ca, Cd, Ce, Co, Cr, Cu, Dy, Er, Eu, Fe, Ga, Gd, Ge, Hf, Ho, In, La, Li, M, Mg, Mn, Mo, Na, Nb, Nd, Ni, O, P, Pb, Pr, Sb, Sc, Si, Sm, Sn, Sr, T, Ta, Tb, Te, Ti, Tm, V, W, Y, Yb, Zn, Zr). It is the proportion of each of these elements found in the ceramic material which forms the input to the network.

In addition to the full dataset described above, an "optimised" dielectric dataset was obtained. This consisted of a subset of the data, selected by removing all glass material and all materials containing unusual dopants. The optimised dataset consists of 90 records containing 37 different elements (Al, Ba, Bi, Ca, Ce, Co, Cu, Eu, F, Fe, Ga, Gd, Ge, Hf, La, Li, M, Mg, Mn, Na, Nb, Nd, Ni, O, Pb, Pr, Si, Sm, Sn, Sr, T, Ta, Ti, V, W, Zn, Zr). Again, the compositional information forms the input to the neural network and the dielectric properties the output.

Our ion-diffusion dataset contains 1100 records of oxygen diffusing materials and their properties. The input data used for mining of the ion-diffusion data mainly consists of the compositional information of each material as in the dielectric dataset. The materials consist of Group II, transition metal, lanthanide and actinide oxides and contain 32 different elements (Al, Ba, Bi, Ca, Cd, Ce, Co, Cr, Cu, Dy, Fe, Ga, Gd, Ho, In, La, Mg, Mn, Nb, Nd, Ni, O, Pr, Sc, Si, Sm, Sr, Ti, V, Y, Yb, Zr). The proportion of these elements, along with the temperature at which the diffusion coefficient was measured from the network inputs. This dataset was collected from published sources. Unlike the records contained in the dielectric dataset, the ion-diffusion data contains many records which are measurements of the same material composition, performed at different temperatures. To differentiate between such measurements, the measurement temperature is included as an input variable of the ANN.

5 Neural network operation

Pre-processing of training data improves training stability and helps to prevent computational over- or underflow. All of the data is scaled so that the mean value is 0 and the standard deviation is 1. In addition to the scaling algorithms, a technique called principal component analysis (PCA) is performed to remove any linear dependence of the input variables [51].

For the dielectric data, principal component analysis (PCA) was used to reduce the dimensionality of the dataset from the original 53 elements to 16 by removing 2% of the variation of the data. Similarly, for the optimised dielectric dataset, PCA reduced the dimensionality from 37 to 21. PCA of the ion-diffusion data allowed the dataset to be reduced from 33 elements to 16 by removing 2% of the variation of the data. The datasets used are randomly selected from the available data. The full set of data was split into three datasets: training, validation and test. As part of the cross-validation analysis, the data was divided into 10 equal size sub-datasets. One of the datasets is used for testing and the remainder is used for training and validation.

The network contains three layers: input, hidden and output. The number of inputs and outputs were determined by the dimensions of the input data and the number of properties that we were aiming to predict. The number of hidden nodes was determined by trial and error and was chosen to be 15 for all three networks (dielectric, optimised dielectric and diffusion). When training was attempted with 10 hidden nodes, the network was not flexible enough to allow the network to learn the relationships, and generalisation was poor. The use of 20 hidden nodes gave a negligible performance increase. The computational requirements of the training process are low; on a 1.6 GHz single processor machine, the training of a 700 record dataset was completed in 3600 epochs and took approximately 1 minute. The ANNs were developed in Matlab [52], making extensive use of the Neural Network Toolbox [53].

Initial attempts to train the neural network using the dielectric dataset resulted in poor generalisation. The dataset contains records with relative permittivities in the 0-1000 range. Especially poor results were obtained when attempting prediction of materials with permittivity greater than 100. Investigation revealed that the number of records with permittivity greater than 100 is far fewer than that in the range 0-100: 91% of the records are in the 0-100 range and the remaining 9% in the range 100-1000. This resulted in the network being unable to accurately learn which material compositions produce relative permittivities greater than 100.

Records associated with materials which exhibit relative permittivity greater than 100 were removed from the dataset. When network training was restarted, the performance of the network improved considerably, allowing accurate generalised predictions of the relative permittivity. However, as mentioned before, statistical techniques are more reliable when interpolating and so, whilst the predictive ability in the 0-100 range increased, extrapolation, predicting relative permittivity greater than 100, is likely to be relatively inaccurate.

The diffusion coefficients of the data in the ion-diffusion dataset vary over a wide range ($\sim$ 4 orders of magnitude) and our initial training attempts resulted in extremely poor accuracy. The data was preprocessed by taking logarithms of the diffusion coefficients which reduced the absolute range of the output data and resulted in much improved ANN performance.

6 Results

The trained neural networks have been used to predict the properties of the materials in the test datasets which have then been compared to the ex-

perimental results. In addition, we have carried out cross-validation analysis of the data. The tables show data from 10 repetitions of 10-fold cross-validation analysis. To measure the overall network performance, we have calculated both RMS and RRS error functions of the test datasets of the 10-fold cross-validation analysis and then calculated the mean of these error functions. The dataset was then re-randomised, and the 10-fold cross validation performed again. Once 10 randomisations were performed, the mean of the error functions of each cross validation was determined. The tables in this section show the results from each cross-validation and the overall mean and standard deviation of these results. The cross-validation ensures that the results are generalised throughout the entire dataset and the multiple randomisations ensure that the results are not due to coincidental randomisation. The overall "mean of mean" values of the error functions give a good indication of the generalisation error and provide the expected accuracy of predictions made using the neural networks.

Finally, some analysis of the materials in each of the cross-validation datasets has been performed. We have attempted to provide a measure of the difference of the test dataset from the training/validation datasets. To calculate this figure, the mean composition of the test dataset and the combined training/validation datasets were calculated. We then calculated the RMS of the difference between the two mean values to show how the materials in the test dataset compare to the materials in the combined training/validation dataset. Test datasets which have a low mean composition difference from the training/validation datasets are more similar to the training/validation data and thus likely to perform better than test datasets with a large mean composition difference.

6.1 Prediction performance of the network trained using the dielectric dataset

The full dielectric dataset was divided into three sub-datasets (training, validation and test) and training was performed until halted by early stopping. The trained network was used to predict the (dimensionless) relative permittivity of the test dataset; the correlation between the experimentally observed permittivity and the predicted permittivity is shown in Figure 1 which demonstrates the accuracy of the predictions. The RMS error of the predicted data compared with the experimental data is 0.61. Figure 1 is a plot of the second dataset combination from the cross-validation analysis.

Statistical analysis of neural networks developed from the dielectric dataset was obtained by performing 10 repetitions of 10-fold cross-validation analysis. Results of this analysis are provided in Table 1 which shows the RMS and RRS error values, the parameters of a straight line fitted using least

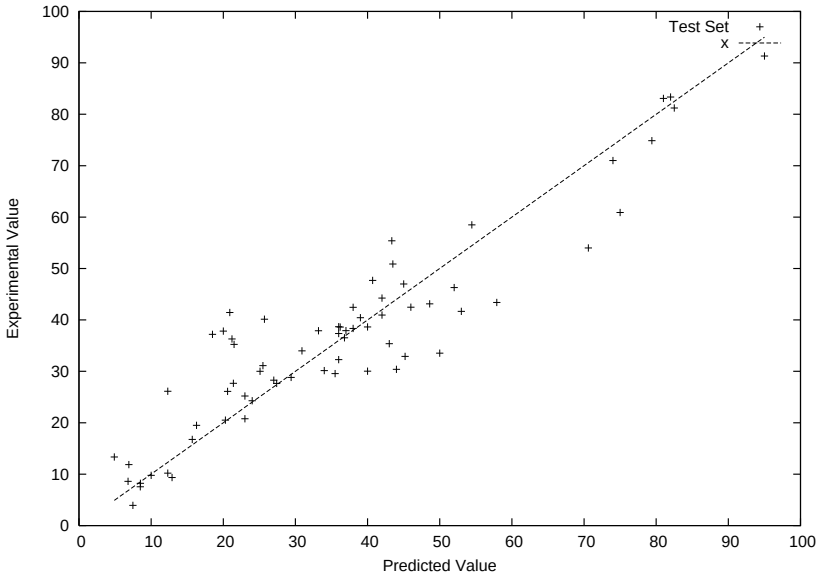

Fig. 1. **The performance of the back-propagation MLP neural network used to predict the permittivity of the test dataset from the full dielectric dataset. This plot illustrates the performance of the second dataset combination in the cross–validation analysis (See Table 1). An ideal straight line with intercept 0 and slope 1 is also shown. The RRS error of the predictions is 0.61.**

squares regression and the RMS of the mean compositional difference between the test dataset and the training/validation dataset. Also included are the the mean and standard deviation of these values. The values obtained are very similar as indicated by the standard deviation which confirms that each of the datasets contains a good representation of the whole dataset. This demonstrates that each sub-dataset is well randomised and the neural network performance is not simply due to the selection of the sub-datasets.

Also shown is a repeated cross-validation analysis of the dielectric dataset with ionic radii data included (Table 2). The ionic radius data was included by calculating the sum of the ionic radii of the elements in the corresponding material, in proportion to their fractional composition. The inclusion of ionic radius data leads to no change in the prediction performance of the network trained using the full dielectric dataset. The RRS error of the predictions remains at 0.6.

Quantity	Dataset randomisation										Mean	Std Dev.
	1	2	3	4	5	6	7	8	9	10		
Intercept	1.05	1.62	0.27	-0.25	2.33	0.75	0.22	1.44	-0.88	-0.02	0.65	0.97
Gradient	0.98	0.96	0.98	1.01	0.96	0.97	1	0.97	1.03	0.99	0.99	0.02
Correlation	0.63	0.63	0.68	0.65	0.64	0.62	0.64	0.65	0.65	0.63	0.64	0.02
RMS Error	13.48	13.42	12.54	13.2	13.34	13.74	13.24	12.83	13.06	13.26	13.21	0.34
RMS mean material difference	0.13	0.14	0.14	0.13	0.13	0.14	0.15	0.13	0.14	0.13	0.14	0.01
RRS Error	0.62	0.62	0.57	0.6	0.61	0.62	0.6	0.58	0.59	0.6	0.6	0.02

Table 1
The performance of the back-propagation MLP neural network used to predict the data within the test datasets taken from the dielectric dataset. Repeated cross-validation analysis was used to obtain these results and the mean and standard deviation are also given.

Quantity	Dataset randomisation										Mean	Std Dev.
	1	2	3	4	5	6	7	8	9	10		
Intercept	0.73	0.39	0.96	0.75	1.57	1.36	-0.65	-0.02	2.21	-1.29	0.6	1.05
Gradient	0.99	0.98	0.99	0.97	0.95	0.96	1.01	1.00	0.96	1.01	0.98	0.02
Correlation	0.65	0.67	0.65	0.63	0.62	0.62	0.67	0.64	0.67	0.68	0.65	0.02
RMS Error	12.91	12.58	13.07	13.54	13.47	13.57	12.77	13.35	12.71	12.48	13.04	0.41
RMS mean material difference	0.15	0.14	0.15	0.14	0.16	0.13	0.13	0.16	0.14	0.14	0.14	0.01
RRS Error	0.59	0.58	0.6	0.62	0.63	0.61	0.58	0.60	0.58	0.57	0.6	0.02

Table 2
The performance of the back-propagation MLP neural network used to predict the data within the test datasets taken from the dielectric dataset. The dataset includes ionic radii as input variables. Repeated cross-validation analysis was used to obtain these results and the mean and standard deviation are also given. Comparison with the data reported in Table 1 shows that inclusion of ionic radius has no effect on the quality of predictions.

6.2 Prediction performance of the network trained using the optimised dielectric dataset

The optimised dielectric dataset was examined in a similar fashion to the full dielectric dataset. The dataset was divided into three, and training carried out using the early stopping technique to prevent over-training. Relative permittivity predictions of the test dataset were again obtained and the networks performance is summarised in Figure 2. This figure shows the accuracy of the neural network predictions compared to those obtained by experiment. The straight line shows the ideal correlation.

As before, network training was performed using cross-validation analysis. The results of this are summarised in Table 3. Again, since the statistical data are similar for each of the trained networks, the datasets each contain a good representation of the whole dataset and the result obtained in Figure 2 is not simply due to the random selection of the datasets.

Also shown is a repeated cross-validation analysis of the optimised dielectric dataset with ionic radius data included (Table 4). As before, the ionic

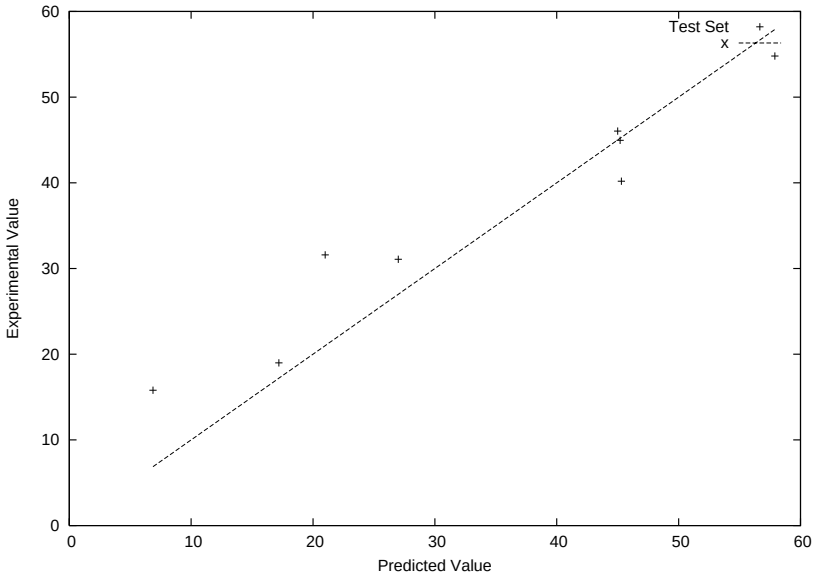

Fig. 2. The performance of the back-propagation MLP neural network used to predict the permittivity of the test dataset from the optimised dielectric dataset. This plot illustrates the performance of the first dataset in the cross-validation analysis (See Table 3). An ideal straight line is shown as in the previous figure. The RRS error between experimental and predicted data is 0.63 (dimensionless).

radius data was included by calculating the sum of the ionic radii of the elements in the material, in proportion to their fractional composition within the material. The inclusion of ionic radii data results in an increase in prediction performance as indicated by the RRS error decrease from 0.71 to 0.65.

Whilst the ANN's predictions agree well with the experimental values in the dataset, it should be remembered that the network uses the experimental results as part of the training process and is therefore itself subject to the error in the experimental data. An ANN will never be able to provide predictions of properties which are more accurate than the error in the experimental measurements. Unfortunately, we do not have any error information for the dielectric data. Since the neural network uses experimental data in the training algorithm, the experimental error represents the intrinsic accuracy of the network. Overall, the network performs better when using the complete rather than the optimised dataset. When only compositional information is included, the RRS error of the cross-validated system is reduced from 0.71 to 0.60 when the entire dataset is used. The standard deviation of the RRS error function obtained from the optimised dataset is larger than for the full dataset, possibly indicating that there is insufficient data for training the network when using the optimised dataset.

As stated earlier, we expect the trained networks to perform well in interpolation, but less reliably in extrapolation. We can attempt to gauge the

Quantity	Dataset randomisation										Mean	Std Dev.
	1	2	3	4	5	6	7	8	9	10		
Intercept	2.24	7.03	0.94	3	-3.18	-4.24	-0.41	1.16	-10.35	2.27	-0.15	4.78
Gradient	0.94	0.85	0.96	0.91	1.05	1.14	0.97	0.88	1.26	1.02	1	0.13
Correlation	0.64	0.44	0.62	0.6	0.61	0.67	0.6	0.51	0.63	0.6	0.59	0.07
RMS Error	13.87	19.23	15.37	14.19	13.71	14.47	15.37	17.33	15.51	15.32	15.44	1.7
RMS mean material difference	0.4	0.38	0.38	0.38	0.42	0.4	0.38	0.4	0.4	0.39	0.39	0.01
RRS Error	0.63	0.89	0.71	0.69	0.63	0.62	0.71	0.76	0.69	0.72	0.71	0.08

Table 3
The performance of the back-propagation MLP neural network used to predict the data within the test datasets taken from the optimised dielectric data. Repeated cross-validation analysis was used to obtain these results and the mean and standard deviation are also given.

Quantity	Dataset randomisation										Mean	Std Dev.
	1	2	3	4	5	6	7	8	9	10		
Intercept	2.01	11.17	1.67	-6.28	0.14	5.26	-13.31	-9.05	-2.14	-3.17	-1.37	7.1
Gradient	0.96	0.75	0.89	1.09	0.99	0.91	1.31	1.2	1.02	1.07	1.02	0.16
Correlation	0.64	0.56	0.57	0.69	0.71	0.57	0.57	0.64	0.73	0.73	0.64	0.07
RMS Error	14.04	15.31	17.46	14.81	12.41	16.07	15.73	14.82	14.63	13.02	14.83	1.46
RMS mean material difference	0.39	0.41	0.38	0.38	0.36	0.40	0.36	0.38	0.39	0.40	0.38	0.02
RRS Error	0.61	0.70	0.74	0.63	0.53	0.75	0.68	0.62	0.65	0.55	0.65	0.07

Table 4
The performance of the back-propagation MLP neural network used to predict the data within the test datasets taken from the optimised dielectric dataset. The dataset includes ionic radius data as a input variable. Repeated cross-validation analysis was used to obtain these results and the mean and standard deviation are also given.

probability that the prediction of the properties of a material are accurate by measuring the "distance" of a material's composition from the hypothetical mean material. If a material is within, say, one standard deviation of the mean, the network is operating close to known parameter space and the predictions obtained are more likely to be accurate than materials which are "further away" in parameter (here composition) space.

6.3 Prediction performance of the network trained using the ion-diffusion dataset

Analysis of the ion-diffusion dataset was performed using the same method as for the dielectric dataset. The dataset was randomised, divided into the three sub-datasets and training carried out until halted by the early stopping technique. The trained network was used to predict the logarithm of the diffusion coefficient (cm^2s^{-1}) of the records in the test dataset. The comparison between the predicted and experimental values is shown in Figure 3 and the RRS error of the predicted data compared to the experimental

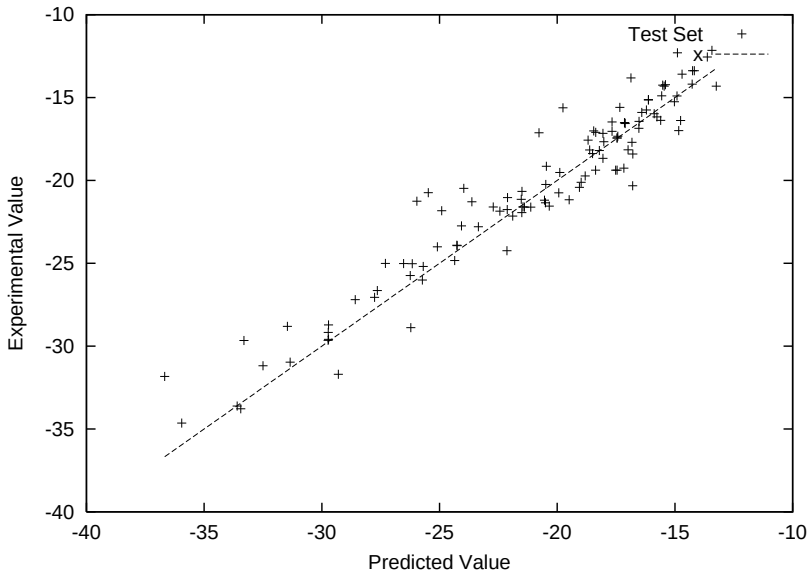

Fig. 3. The performance of the back-propagation MLP neural network used to predict the diffusion coefficient (cm^2s^{-1}) of the test dataset from the ion-diffusion dataset. The RMS error between experimental and predicted data is 0.34 (dimensionless, since the network is trained using the logarithm of the diffusion data).

data is 2.12 (dimensionless since we are working with the logarithm of the diffusion coefficient).

As for the dielectric dataset, it should be remembered that the network uses the experimental results as part of the training process and is subject to the error in the data. An ANN will never be able to provide predictions of properties which are more accurate than the error in the experimental measurements. Unfortunately, the ion-diffusion dataset only contains errors for about 3% of the records. Due to the lack of error information, we are unable to perform comparisons between the ANN and experimental data and thus to determine whether or not the ANN predicts values within experimental error. As before, repeated cross-validation analysis was performed. The results of this are summarised in Table 5. The low standard deviation of the mean values shows that each of the datasets contains a good representation of the whole dataset and the result obtained in Figure 3 is not simply a coincidence of the randomisation and selection of the datasets. Again, interpolated predictions are more likely to be accurate than extrapolated results and we can use compositional distances from the mean composition to attempt to predict the expected accuracy of our predictions.

Quantity	Dataset randomisation										Mean	Std Dev.
	1	2	3	4	5	6	7	8	9	10		
Intercept	-0.07	-0.04	-0.12	0.23	-0.29	0.05	-0.05	0.37	0.14	0.21	0.04	0.2
Gradient	1	1	1	1.01	0.99	1.01	1	1.01	1.01	1.01	1	0.01
Correlation	0.88	0.88	0.88	0.87	0.86	0.88	0.88	0.89	0.87	0.87	0.88	0.01
RMS Error	2.12	2.07	2.1	2.13	2.26	2.08	2.1	2.04	2.14	2.15	2.12	0.06
RMS mean material difference	0.11	0.11	0.11	0.1	0.11	0.11	0.11	0.12	0.12	0.11	0.11	0.01
RRS Error	0.35	0.34	0.34	0.35	0.37	0.34	0.34	0.34	0.35	0.35	0.35	0.01

Table 5
The performance of the back-propagation ANN on the ion-diffusion dataset. Repeated cross-validation analysis was used to obtain these results and the mean and standard deviation are also given.

6.4 Radial basis function networks

In contrast to MLP networks detailed in the previous section, attempted training of radial basis function networks resulted in networks which generalised poorly. After making attempts to train networks using spherical RBFs, using the K-means clustering algorithm, we proceeded to modify the code to allow ellipsoidal basis functions which unfortunately resulted in no improvement. A possible reason for the failure of RBF networks to predict the materials properties in this study is that RBF networks perform poorly when there are input variables which have significant variance, but which are uncorrelated with the output variable [8]. MLP networks learn to ignore the irrelevant inputs whilst RBF networks require a large number of hidden units to achieve accurate predictions.

7 Conclusions

Through application of artificial neural networks to pre-existing datasets culled from the literature, we have demonstrated that we can predict the permittivities and diffusion coefficients of ceramic materials simply from their composition and, in the case of the diffusion coefficient, experimental measurement temperature. A three layer perceptron network was trained using the back-propagation algorithm and cross-validation analysis of the data gave a mean root relative squared error of 0.6 for prediction of the dielectric constant of materials in the full dielectric dataset compared to 0.71 for the smaller, optimised dataset. These results agree with previous work in the field of oilfield cements [9] where neural network predictions were substantially enhanced when additional data records were included. The inclusion of ionic radius data results in no change to the prediction accuracy for the full dataset, although, a decrease in root relative squared error of 0.06 was found when the ionic radius data was included in the optimised dielectric dataset. The same network trained using the ion diffusion dataset was able to predict the logarithm of the oxygen diffusion coefficient with a

RRS error of 0.35.

Reliable Baconian methods for the prediction of the properties of ceramic materials are likely to become powerful tools for the scientific community whose accuracy will increase as more data is generated. The data produced by the FOXD project [20,24] is beginning to accumulate and will be used to further develop these artificial neural networks. Through the use of evolutionary optimisation techniques such as the genetic algorithms of Holland [54], we hope to be able to invert the neural networks described in this paper [9]. This inversion provides the ability to search for materials with desirable properties which can then be synthesised using the London University Search Instrument. Other data mining tools including rule induction algorithms such as C4.5 [55] can also be used to provide explicit, meaningful performance prediction rules from neural networks [56].

As part of the larger FOXD project, artificial neural networks akin to those developed here will form a vital link in the materials discovery cycle, leading to the possibility of steering automated searches in the compositional search space. In addition to producing data for further artificial neural network studies, ultimately we hope to use these techniques to discover and investigate new materials suitable for use in telecommunications, fuel cell and other areas.

8 Acknowledgements

We wish to thank Simon Clifford for fruitful discussions and Rob Pullar for dielectric property information. We would also like to express our thanks to Professor Julian Evans, Shoufeng Yang, Lifeng Chen and Yong Zhang at Queen Mary College, University of London.

This research is supported by the EPSRC-funded project "Discovery of New Functional Oxides by Combinatorial Methods" (GR/S85269/01) [24]. Copies of the software and literature datasets described herein may be obtained upon application to the authors.

References

[1] W. D. Kingery, H. K. Bowen, U. D. R., Introduction To Ceramics, John Wiley and Sons Ltd, 1976.

[2] K. R. Popper, Conjectures and Refutations, Routledge and Kegan Paul plc, 1963.

[3] F. Bacon, Novum Organum, in the Philosophical Works of Francis Bacon, Routeledge, London, 1905.

[4] J. C. H. Rossini, S. Fearn, J. A. Kilner, D. J. Scott, M. J. Harvey, Modelling and database issues addressed to the search for mixed oxygen ionic conductors by combinatorial methods, in: Proceedings of the 7th European Solid Oxide Fuel Cell Forum, Lucerne, Switzerland, 2006.

[5] A. Ali, K. Nandakumar, J. Luo, K. T. Chuang, A novel approach to study the structure versus performance relationship of SOFC cathodes, Journal of Power Sources In press.

[6] W. Preis, W. Sitte, Modelling of grain boundary resistivities of n-conducting $BaTiO_3$ ceramics, Solid State Ionics In press.

[7] J. Gasteiger, J. Zupan, Neural Networks in Chemistry, Angewandte Chemie International Edition 32 (4) (1993) 503–527.

[8] C. M. Bishop, Neural Networks for Pattern Recognition, Oxford University Press, 1995.

[9] P. V. Coveney, P. Fletcher, T. L. Hughes, Using artificial neural networks to predict the quality and performance of oil-field cements, AI Magazine 17 (4) (1996) 41–53.

[10] P. V. Coveney, W. Humphries, Molecular modelling of the mechanism of action of phosphonate retarders on hydrating cements, Journal of the Chemical Society, Faraday Transactions 92 (1996) 831–841.

[11] T. Masters, Practical Neural Network Recipes in C++, Academic Press, 1993.

[12] I. A. Basheer, M. Hajmeer, Artificial neural networks: fundamentals, computing, design, and application, Journal of Microbiological Methods 43 (2000) 3–31.

[13] D. Guo, Y. Wang, J. Xia, C. Nan, L. Li, Investigation of $BaTiO_3$ formulation: an artificial neural network (ANN) method, Journal of the European Ceramic Society 22 (2002) 1867–1872.

[14] I. Kuzmanovski, S. Aleksovska, Optimization of artificial neural networks for prediction of the unit cell parameters in orthorhombic perovskites. comparison with multiple linear regression, Chemometrics and Intelligent Laboratory Systems 67 (2) (2003) 167–174.

[15] L. Chonghe, T. Yihao, Z. Yingzhi, W. Chunmei, W. Ping, Prediction of lattice constant in perovskites of $GdFeOb_3$ structure, Journal of Physics and Chemistry of Solids 64 (11) (2003) 2147–2156.

[16] D. Guo, L. Li, C. Nan, J. Xia, Z. Gui, Modeling and analysis of the electrical properties of PZT through neural networks, Journal of the European Ceramic Society 23 (2003) 2177–2181.

[17] S. Sild, M. Karelson, A General QSPR Treatment for Dielectric Constants of Organic Compounds, Journal of Chemical Information and Modelling 42 (2) (2002) 360–367.
URL http://dx.doi.org/10.1021/ci010335f

[18] R. Guha, P. C. Jurs, Interpreting Computational Neural Network QSAR Models: A Measure of Descriptor Importance, Journal of Chemical Information and Modelling 45 (2005) 600–806.

[19] R. C. Schweitzer, J. B. Morris, Development of a quantitative structure property relationship (QSPR) for the prediction of dielectric constants using neural networks, Analytical Chimica Acta 384 (1999) 285–303.

[20] M. J. Harvey, D. Scott, P. V. Coveney, An integrated instrument control and informatics system for combinatorial materials research, Journal of Chemical Information and Modelling 46 (2005) 1026–1033.

[21] A. J. Moulson, J. M. Herbert, Electroceramics, John Wiley and Sons Ltd, 2003.

[22] J. R. G. Evans, M. J. Edirisinghe, P. V. Coveney, J. Eames, Combinatorial searches of inorganic materials using the ink-jet printer: science, philosophy and technology, Journal of the European Ceramic Society 21 (2001) 2291–2299.

[23] E. W. McFarland, W. H. Weinberg, Combinatorial approaches to materials discovery, Trends in Biotechnology 17 (1999) 107–115.

[24] Functional OXide Discovery, EPSRC Grant: GR/S85269/01.
URL http://www.foxd.org

[25] W. Wersing, Microwave ceramics for resonators and filters, Current Opinion in Solid State and Materials Science 1 (1996) 715–731.

[26] H. V. Alexandru, C. Berbecaru, A. Ioachim, M. I. Toacsen, M. G. Banciu, L. Nedelcu, D. Ghetu, Oxides ferroelectric $BaSrTiO_3$ for microwave devices, Materials Science and Engineering B 109 (2004) 152–159.

[27] H. V. Alexandru and C. Berbecaru and F. Stanculescu and A. Ioachim and M. G. Banciu and M.I. Toacsen and L. Nedelcu and D. Ghetu and G. Stoica, Ferroelectric solid solutions (Ba,Sr)TiO_3 for microwave applications, Materials Science and Engineering B 118 (2005) 92–96.

[28] A. Ioachim, R. Ramer, M. I. Toacsan, M. G. Banciu, L. Nedelcu, C. A. Dutu, F. Vasiliu, H. V. Alexandru, C. Berbecaru, G. Stoica, P. Nita, Ferroelectric ceramics based on the BaO-SrO-TiO_2 ternary system for microwave applications, Journal of the European Ceramic Society In press.

[29] J.-H. Jeon, Effect of $SrTiO_3$ concentration and sintering temperature on microstructure and dielectric constant of $Ba_{1-x}Sr_xTiO_3$, Journal of the European Ceramic Society 24 (2004) 1045–1048.

[30] D. Guo, Y. Wang, C. Nan, L. Li, J. Xia, Application of artificial neural network technique to the formulation design of dielectric ceramics, Sensors and Actuators A 102 (2002) 93–98.

[31] K. Cai, J. Xia, L. L. Z. Gui, Analysis of the electrical properties of PZT by a BP artificial neural network, Computational Materials Science 34 (2005) 166–172.

[32] S. J. Skinner, J. A. Kilner, Oxygen ion conductors, Materials Today 6 (2003) 30–37.
URL
http://www.sciencedirect.com/science/article/B6X1J-47XMC8S-14/2/db80a06d4701

[33] N. P. Bansal, Z. Zhong, Combustion Synthesis of $Sm_{0.5}Sr_{0.5}CoO_{3-x}$ and $La_{0.6}Sr_{0.4}CoO_{3-x}$ nanopowders for solid oxide fuel cell cathodes, Journal of Power Sources 158 (2006) 148–153.

[34] S. Fearn, J. C. H. Rossiny, J. A. Kilner, Y. Zhang, L. Chen, High throughput screening of novel oxide conductors using sims, Applied Surface Science 252 (2006) 7159–7162.
URL
http://www.sciencedirect.com/science/article/B6THY-4JYKMJP-2/2/8c2db6e474678

[35] M.-H. Hung, M. V. M. Rao, D.-S. Tsai, Microstructures and electrical properties of calcium substituted $LaFeO_3$ as SOFC cathode, Materials Chemistry and Physics In Press.
URL
http://www.sciencedirect.com/science/article/B6TX4-4K9C521-1/2/1ddcb15816717

[36] S. J. Skinner, J. A. Kilner, Oxygen diffusion and surface exchange in $La_{2-x}Sr_xNiO_{4+\delta}$, Solid State Ionics 135 (2000) 709–712.

[37] Q. Zhu, T. Jin, Y. Wang, Thermal expansion behavior and chemical compatibility of $Ba_xSr_{1-x}Co_{1-y}Fe_yO_{3-\delta}$ with 8YSZ and 20GDC, Solid State Ionics 177 (2006) 1199–1204.
URL
http://www.sciencedirect.com/science/article/B6TY4-4K48N76-2/2/c394a5f943c31

[38] S. O. T. Ogaji, R. Singh, P. Pilidis, M.Diacakis, Modelling fuel cell performance using artificial intelligence, Journal of Power Sources 154 (2006) 192–197.

[39] J. Arriagada, P. Olausson, A. Selimovic, Artificial neural network simulator for SOFC performance prediction, Journal of Power Sources 112 (2002) 54–60.

[40] W.-Y. Lee, G.-G. Park, T.-H. Yang, Y.-G. Yoon, C.-S. Kim, Emperical modelling of polymer electrolyte membrane fuel cell performance using artificial neural networks, International Journal of Hydrogen Energy 29 (2004) 961–966.

[41] S. Ou, L. E. K. Achenie, A hybrid neural network for PEM fuel cells, Journal of Power Sources 140 (2005) 319–330.

[42] V. A. Gotlib, T. Sato, A. I. Beltzer, Neural computing of effective properties of random composite materials, Computers and Structures 79 (2001) 1–6.

[43] H. Saxén, F. Pettersson, Method for the selection of inputs and structure of feedforward neural networks, Computers and Chemical Engineering 30 (2006) 1038–1045.

[44] B. Curry, P. H. Morgan, Model Selection in Neural Networks: Some difficulties, European Journal of Operational Research 170 (2006) 567–577.

[45] R. Hecht-Nielsen, Theory of the Backpropagation Neural Network, Proceedings of the International Joint Conference on Neural Networks (1989) 593–603.

[46] Y. A. Alsultanny, M. M. Aqul, Pattern recognition using multilayer neural-genetic algorithm, Neurocomputing 51 (2003) 237–247.

[47] M. J. D. Powell, Algorithms for Approximation, Oxford:Clarendon Press, 1987.

[48] J. Moody, C. J. Darken, Fast learning in networks of locally-tuned processing units, Neural Computation 1 (1989) 281–295.

[49] T. M. Mitchell, Machine Learning, McGraw-Hill, 1997.

[50] M. T. Sebastian, A.-K. Axelsson, N. M. N. Alford, List of microwave dielectric resonator materials and their properties, London South Bank University - Physical Electronics and Materials group.
URL `http://www.lsbu.ac.uk/dielectric-materials/`

[51] G. H. Dunteman, Principal Component Analysis, Sage Publications, 1989.

[52] Mathworks, Matlab (1984-2000).
URL `http://www.mathworks.com/products/matlab/`

[53] Matlab Neural Network Toolbox.
URL `http://www.mathworks.com/products/neuralnet/`

[54] J. Holland, Adaptation in Natural and Artificial Systems, University of Michigan Press, Ann Arbor, USA, 1975.

[55] J. R. Quinlan, Programs for Machine Learning, Morgan Kaufmann, San Fransisco, USA, 1993.

[56] G. G. Towell, J. W. Shavlik, Extracting refined rules from knowledge-based neural networks, Machine Learning 13 (1993) 71–101.